

# Simultaneous Transmitting and Reflecting (STAR)-RIS for Harmonious Millimeter Wave Spectrum Sharing

Omar Hashash<sup>1</sup>, Walid Saad<sup>1</sup>, Mohammadreza F. Imani<sup>2</sup>, and David R. Smith<sup>3</sup>

<sup>1</sup>Wireless@VT, Bradley Department of Electrical and Computer Engineering, Virginia Tech, Arlington, VA, USA.

<sup>2</sup>School of Electrical, Computer and Energy Engineering, Arizona State University, Tempe, AZ, USA.

<sup>3</sup>Department of Electrical and Computer Engineering, Duke University, Durham, NC, USA.

Emails: {omarnh, walids}@vt.edu, mohammadreza.imani@asu.edu, drsmith@duke.edu

**Abstract**—The opening of the millimeter wave (mmWave) spectrum bands for 5G communications has motivated the need for novel spectrum sharing solutions at these high frequencies. In fact, reconfigurable intelligent surfaces (RISs) have recently emerged to enable spectrum sharing while enhancing the incumbents' quality-of-service (QoS). Nonetheless, co-existence over mmWave bands remains persistently challenging due to their unfavorable propagation characteristics. Hence, initiating *mmWave spectrum sharing* requires the RIS to further assist in improving the QoS over mmWave bands without jeopardizing spectrum sharing demands. In this paper, a novel *simultaneous transmitting and reflecting RIS (STAR-RIS)*-aided solution to enable mmWave spectrum sharing is proposed. In particular, the transmitting and reflecting abilities of the STAR-RIS are leveraged to tackle the mmWave spectrum sharing and QoS requirements *separately*. The STAR-RIS-enabled spectrum sharing problem between a primary network (e.g. a radar transmit-receive pair) and a secondary network is formulated as an optimization problem whose goal is to maximize the downlink sum-rate over a secondary multiple-input-single-output (MISO) network, while limiting interference over a primary network. Moreover, the STAR-RIS response coefficients and beamforming matrix in the secondary network are jointly optimized. To solve this non-convex problem, an alternating iterative algorithm is employed, where the STAR-RIS response coefficients and beamforming matrix are obtained using the successive convex approximation method. Simulation results show that the proposed solution outperforms conventional RIS schemes for mmWave spectrum sharing by achieving a 14.57% spectral efficiency gain.

## I. INTRODUCTION

The use of millimeter wave (mmWave) frequencies is a cornerstone of current and future wireless cellular systems [1]. By leveraging the available bandwidth at mmWave frequencies, one can enable a plethora of applications ranging from virtual reality to unmanned aerial vehicles [2]. However, mmWave frequencies are already being used to support existing services such as radar systems [3]. As such, enabling mmWave in beyond 5G (B5G) systems requires novel mechanisms for spectrum sharing between incumbent services and new B5G applications. Meanwhile, co-existence at these high frequencies faces multiple challenges that range from severe signal attenuation to blockage susceptibility which limit mmWave signal propagation [4]. Henceforth, enabling *mmWave spectrum sharing* for B5G applications will require effective schemes that promote mmWave signal propagation and fulfill spectrum sharing demands *simultaneously* [5].

This research was supported by the U.S. National Science Foundation under Grants CNS-2030215 and CNS-2030068.

To tackle these requirements, one can deploy reconfigurable intelligent surfaces (RISs) that have demonstrated a promising potential at mmWave bands [6]. In general, RISs allow adjustment of the propagation environment by inducing amplitude and phase responses on incident wireless signals. Despite the abundance of literature on the use of RISs to enhance the quality-of-service (QoS) at mmWave bands [7], remarkably, only few works look at their use for spectrum sharing between primary and secondary networks [8]–[12]. For spectrum sharing, the RIS can modify the received signals in both primary and secondary networks to control interference levels and enhance spectral efficiency, respectively. For instance, the work in [8] studies a downlink transmit power minimization problem for an RIS-enhanced cognitive radio (CR) system to enable primary-secondary networks co-existence. The authors in [9] investigate the deployment of multiple RISs to maximize the data rate over a multiple-input-single-output (MISO)-CR network. In [10], the authors propose an RIS-enabled successive interference cancellation scheme to enable energy efficient spectrum sharing between transceiver pairs. Moreover, the work in [11] uses an RIS to maximize the detection probability of a radar that co-exists with a secondary network, as per the federal communications commission (FCC) recommendations [12].

Although the works in [8]–[12] showcase diverse applications of RISs for spectrum sharing, tailoring such solutions to the mmWave regime requires further emphasizing the role of the RIS in the interplay between spectrum sharing and propagation enhancement. Despite its essential application in mitigating potential co-existence interference, the RIS plays an indispensable role in overcoming the critical propagation challenges and enhancing the QoS in the mmWave bands. Hence, the RIS is a crucial contributor on both fronts. Nevertheless, enhancing the QoS and mitigating co-existence interference are *tied up to the same RIS phase shifts*. Thus, the achieved phase shifts represent a compromise between both disjoint tasks. This can limit the individual performance on each front and prevent the RIS-based spectrum sharing scheme from reaching the full potential anticipated at mmWave frequencies. *In essence, enabling RIS-based mmWave spectrum sharing solutions necessitates decoupling interference mitigation from QoS enhancement to explore the full mmWave experience in B5G networks, an aspect that was not studied in [8]–[12].*

The main contribution of this paper is a novel *simultaneous transmitting and reflecting reconfigurable intelligent surface*

(STAR-RIS)-aided mmWave spectrum sharing solution for 5G networks. Distinct from conventional reflecting RISs, STAR-RISs can transmit and reflect the incident signals simultaneously, which divides the network into transmitting and reflecting regions accordingly [13]. As each of the primary and secondary networks settle in a particular region, the transmitting and reflecting phase shifts can be employed to *separately* limit co-existence interference and enhance the QoS at mmWave bands. In particular, we consider a primary MISO network to operate over a licensed mmWave band. In this system, we also have a secondary MISO network that comprises user equipments (UEs) operating under the coverage of a base station (BS) and function over the same mmWave band as that of the primary network. To fulfill the demands of both networks, we formulate a spectrum co-existence problem whose goal is to maximize the downlink sum-rate over the secondary network while limiting interference at the primary receiver. As such, the STAR-RIS transmission and reflection coefficients along with the beamforming matrix at the secondary BS are jointly optimized. To solve this non-convex problem, we use an iterative alternating optimization algorithm that allows us to obtain the STAR-RIS response coefficients and beamforming matrix using the successive convex approximation (SCA) method. *To the best of our knowledge, this is the first work to leverage the transmitting and reflecting abilities of a STAR-RIS to separately address the QoS and interference requirements of mmWave spectrum sharing.* Simulation results demonstrate the advantages of replacing conventional RISs with STAR-RISs for mmWave spectrum sharing with a 14.57% gain in spectral efficiency.

The rest of the paper is organized as follows. Section II presents the system model of the STAR-RIS-aided mmWave spectrum sharing system. The iterative alternating algorithm used to optimize the STAR-RIS coefficients and the beamforming matrix is presented in Section III. Simulation results are presented in Section IV, and conclusions are drawn in Section V.

## II. SYSTEM MODEL

### A. Communication Model

Consider a MISO system composed of a primary transmitter (Tx)-receiver (Rx) pair that operate over a licensed mmWave band, as shown in Fig. 1. We assume that the Tx is equipped with multiple antennas, and it communicates with a single antenna Rx. In this network, there exists a secondary multi-user MISO communication network consisting of a BS equipped with  $M$  directional antennas that serves a set  $\mathcal{K}$  of  $K$  single antenna users in the downlink over the same mmWave band. To assist the secondary network downlink communication and limit the possible interference that may result on the primary network, a STAR-RIS having  $N$  equally spaced passive reflecting/transmitting elements is deployed while dividing its surroundings into transmission and reflection regions. Here, we assume that the primary network exists in the transmission region of the STAR-RIS while the secondary UEs exist in the reflective region. In this scenario, the transmitting

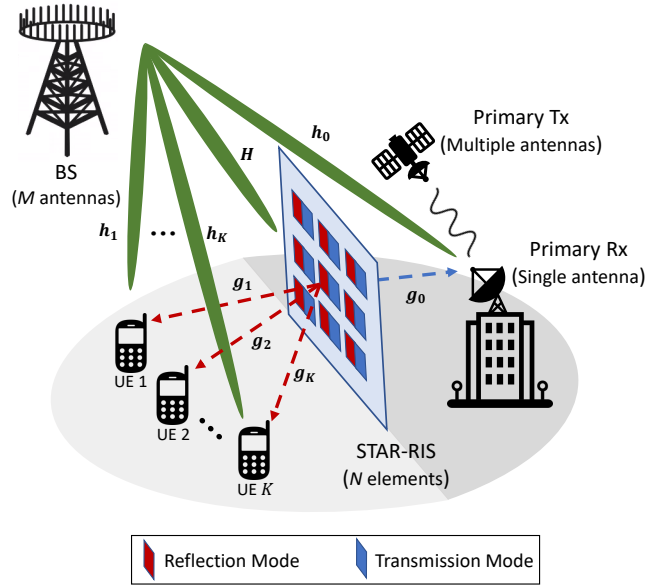


Fig. 1: System model of the wireless network with STAR-RIS-aided mmWave spectrum sharing for primary and secondary networks co-existence.

abilities of the STAR-RIS are dedicated to limit interference in the primary network, while the reflecting abilities assist in the secondary downlink communication. Let  $\mathbf{h}_0 \in \mathbb{C}^{M \times 1}$  be the channel gain between the BS and the primary Rx,  $\mathbf{h}_k \in \mathbb{C}^{M \times 1}$  be the channel gain between the BS and each UE  $k \in \mathcal{K}$ , and  $\mathbf{H} \in \mathbb{C}^{N \times M}$  be the channel matrix between the BS and the STAR-RIS. We also define  $\mathbf{g}_0 \in \mathbb{C}^{N \times 1}$  as the channel gain between the STAR-RIS and primary Rx, and  $\mathbf{g}_k \in \mathbb{C}^{N \times 1}$  as the channel gain between each STAR-RIS element  $n \in \mathcal{N} \triangleq \{1, \dots, N\}$  and UE  $k$ .

In order to initiate downlink communication with multiple UEs, the BS precodes the transmit signal as an  $M \times 1$  vector  $\mathbf{s} = \sum_{k=1}^K \mathbf{w}_k s_k$ , where  $\mathbf{w}_k \in \mathbb{C}^{M \times 1}$  and  $s_k$  are, respectively, the beamforming vector and the unit-power information symbol for each UE  $k \in \mathcal{K}$ . The power allocation of the BS is subject to a maximum power constraint such that  $\|\mathbf{s}\|^2 = \sum_{k \in \mathcal{K}} \|\mathbf{w}_k\|^2 \leq P_{\max}$ , where  $P_{\max}$  is the maximum transmit power of the BS.

From the STAR-RIS operating modes presented in [14], the energy splitting (ES) mode is favored as it can simultaneously provide operations over both regions. Hence, to characterize the ES mode for the STAR-RIS, we consider that the energy of the signal incident on each RIS element  $n$  is subject to transmission and reflection by assuming that the elements can support electric and magnetic currents [13]. Accordingly, the transmission and reflection coefficients of element  $n$  can be expressed as  $T_n = \sqrt{\beta_n^t} e^{j\theta_n^t}$  and  $R_n = \sqrt{\beta_n^r} e^{j\theta_n^r}$  respectively, where  $\sqrt{\beta_n^t} \in [0, 1]$ ,  $\sqrt{\beta_n^r} \in [0, 1]$ ,  $\theta_n^t \in [0, 2\pi)$ , and  $\theta_n^r \in [0, 2\pi)$  are, respectively, the amplitude and phase response of the transmission and reflection coefficient of the  $n$ th element. The phase responses  $\theta_n^t$  and  $\theta_n^r$  can be adjusted independently, while the amplitude response of the transmission and reflection coefficients for each element  $n$  is governed by the law of

conservation of energy such that  $|T_n|^2 + |R_n|^2 = 1$  [14]. Here, we assume that the passive STAR-RIS elements are ideal with negligible energy consumption. This leads to the following condition:  $\beta_n^t + \beta_n^r = 1$ .

The transmission coefficient matrix of the STAR-RIS is given by  $\Theta_t = \text{diag}(T_1, T_2, \dots, T_N)$ . Similarly, the reflection coefficient matrix is given by  $\Theta_r = \text{diag}(R_1, R_2, \dots, R_N)$ . Then, we can define the signal at the primary Rx as  $y = x + (\mathbf{h}_0^H + \mathbf{g}_0^H \Theta_t \mathbf{H})\mathbf{s} + n_0$ , where  $x \in \mathbb{C}$  is the received primary signal and  $n_0 \sim \mathcal{CN}(0, \sigma_0^2)$  is the additive white Gaussian noise at the Rx.

In order to effectively separate the propagation environment from the STAR-RIS response, we re-arrange the received signal at the primary Rx equivalently as:

$$y = x + (\mathbf{h}_0^H + \phi_t^T \mathbf{G}_0)\mathbf{s} + n_0, \quad (1)$$

where  $\phi_t = [T_1, T_2, \dots, T_N]^T \in \mathbb{C}^{N \times 1}$  is the transmission coefficients vector and  $\mathbf{G}_0 = \text{diag}(\mathbf{g}_0^H)\mathbf{H} \in \mathbb{C}^{N \times M}$  is the cascaded BS-RIS-Rx transmission channel response while removing the effect of the STAR-RIS. The corresponding signal-to-interference-plus-noise (SINR) ratio at the primary Rx will then be:

$$\gamma(\mathbf{W}, \phi_t) = \frac{P_{\text{Rx}}}{\sum_{k=1}^K |(\mathbf{h}_0^H + \phi_t^T \mathbf{G}_0)\mathbf{w}_k|^2 + \sigma_0^2}, \quad (2)$$

where  $P_{\text{Rx}} = \mathbb{E}[|x|^2]$  is the received primary signal power at the primary Rx and  $\mathbf{W} = [\mathbf{w}_1, \dots, \mathbf{w}_K] \in \mathbb{C}^{M \times K}$  is the beamforming matrix at the BS. Similarly, we define the received signal at UE  $k$  as:

$$y_k = (\mathbf{h}_k^H + \mathbf{g}_k^H \Theta_r \mathbf{H})\mathbf{s} + n_k = (\mathbf{h}_k^H + \phi_r^T \mathbf{G}_k)\mathbf{s} + n_k, \quad (3)$$

where  $n_k \sim \mathcal{CN}(0, \sigma_k^2)$  is the additive white Gaussian noise at UE  $k$ ,  $\phi_r = [R_1, R_2, \dots, R_N]^T \in \mathbb{C}^{N \times 1}$  is the reflection coefficients vector, and  $\mathbf{G}_k = \text{diag}(\mathbf{g}_k^H)\mathbf{H}$  is the cascaded BS-RIS-UE reflection channel response while removing the effect of the STAR-RIS. We assume that no interference occurs from the primary network to the secondary as the primary Tx-Rx pair provides a point-to-point service and any power received at the UE from the primary network can be considered to be negligible. This assumption is reasonable because the primary Rx has a static position and receives a narrow beamwidth signal. Hence, we can then assume that the signal arriving at each UE  $k$  is subject to composite channel interference.

As a result, we can define the total sum-rate for all UEs as:

$$r(\mathbf{W}, \phi_r) = \sum_{k=1}^K B \log_2 \left( 1 + \frac{|(\mathbf{h}_k^H + \phi_r^T \mathbf{G}_k)\mathbf{w}_k|^2}{\sum_{\substack{i=1 \\ i \neq k}}^K |(\mathbf{h}_k^H + \phi_r^T \mathbf{G}_k)\mathbf{w}_i|^2 + \sigma_k^2} \right), \quad (4)$$

where  $B$  is the channel bandwidth.

### B. Problem Formulation

Our main objective is to optimize the beamforming matrix at the BS and the transmission and reflection coefficients of the STAR-RIS so as to maximize the sum-rate over the secondary network, while ensuring that the interference experienced by the primary network is maintained below a minimum threshold. It is assumed that perfect channel state information

(CSI) are available at the BS. Hence, we can now define our problem:

$$\max_{\mathbf{W}, \phi_t, \phi_r} r(\mathbf{W}, \phi_r) \quad (5a)$$

$$\text{subject to } \gamma(\mathbf{W}, \phi_t) \geq \gamma_{\min}, \quad (5b)$$

$$\sum_{k=1}^K \|\mathbf{w}_k\|^2 \leq P_{\max}, \quad (5c)$$

$$\beta_n^t + \beta_n^r = 1 \quad \forall n \in \mathcal{N}, \quad (5d)$$

$$\beta_n^t, \beta_n^r \in [0, 1] \quad \forall n \in \mathcal{N}, \quad (5e)$$

$$\theta_n^t, \theta_n^r \in [0, 2\pi) \quad \forall n \in \mathcal{N}, \quad (5f)$$

where  $\gamma_{\min}$  is the minimum SINR required for the primary Rx to decode the signal  $x$  successfully. The objective function in (5a) is the sum-rate of the secondary network users in the downlink. The minimum SINR requirement for decoding at the primary Rx is given in (5b). The power budget on the BS is captured by (5c). The law of conservation of energy that governs the relationship between the amplitude response of the transmission and reflection coefficient is given in (5d). This problem showcases the novelty behind integrating a STAR-RIS for spectrum sharing, as it can solely provide a simultaneous solution to separately increase spectral efficiency and limit interference through two independent phase shift coefficients. Hence, the STAR-RIS provides additional degrees of freedom for spectrum sharing by leveraging both transmitting and reflecting abilities in comparison to conventional RISs with single-sided reflection. However, this comes at the expense of compromising the unity amplitude response of conventional RISs with reduced amplitude responses of STAR-RISs.

The objective function in (5a) is non-convex and it is difficult to obtain a global optimal solution. In the next section, we propose an iterative algorithm by using alternating optimization to determine a sub-optimal solution of the beamforming matrix at the BS and the STAR-RIS transmitting and reflecting coefficients.

### III. ALTERNATING OPTIMIZATION FOR BEAMFORMING MATRIX AND STAR-RIS COEFFICIENTS

In this section, the beamforming matrix at the BS and the STAR-RIS transmission and reflection coefficients are jointly optimized to solve problem (5). We can fix the values of  $\mathbf{W}$ , and  $\phi_t$  and  $\phi_r$  alternatively, and solve the problem through an iterative procedure.

#### A. STAR-RIS Transmission and Reflection Coefficients Optimization

For a fixed value of  $\mathbf{W}$ , the problem in (5) reduces to an optimal transmission and reflection coefficients optimization problem as follows:

$$\max_{\rho, \phi_t, \phi_r} r(\phi_r) = \sum_{k=1}^K B \log_2(1 + \rho_k) \quad (6a)$$

$$\text{subject to } \rho_k \leq \frac{|(\mathbf{h}_k^H + \phi_r^T \mathbf{G}_k)\mathbf{w}_k|^2}{\sum_{i=1, i \neq k}^K |(\mathbf{h}_k^H + \phi_r^T \mathbf{G}_k)\mathbf{w}_i|^2 + \sigma_k^2}, \quad (6b)$$

$$\sum_{k=1}^K |(\mathbf{h}_0^H + \phi_t^T \mathbf{G}_0)\mathbf{w}_k|^2 + \sigma_0^2 \leq \frac{P_{\text{Rx}}}{\gamma_{\min}}, \quad (6c)$$

$$(5d), (5e), (5f), \quad (6d)$$

where  $\boldsymbol{\rho} = [\rho_1, \rho_2, \dots, \rho_K]$  is a slack vector which ensures that constraint (6b) will always hold with equality to the optimal solution. Constraint (6c) guarantees that the interference at the primary Rx is below threshold. We now define  $\tilde{\mathbf{g}}_{kk} = (\mathbf{G}_k \mathbf{w}_k)^*$ ,  $\tilde{\mathbf{g}}_{ki} = (\mathbf{G}_k \mathbf{w}_i)^*$ , and  $\tilde{\mathbf{g}}_{0k} = (\mathbf{G}_0 \mathbf{w}_k)^*$ , and, then, (6b) and (6c) can be written as:

$$\rho_k \leq \frac{|\tilde{h}_{kk} + \tilde{\mathbf{g}}_{kk}^H \boldsymbol{\phi}_r|^2}{\sum_{i=1, i \neq k}^K |\tilde{h}_{ki} + \tilde{\mathbf{g}}_{ki}^H \boldsymbol{\phi}_r|^2 + \sigma_k^2}, \quad (7)$$

$$\sum_{k=1}^K |\tilde{h}_{0k} + \tilde{\mathbf{g}}_{0k}^H \boldsymbol{\phi}_t|^2 + \sigma_0^2 \leq \frac{P_{\text{Rx}}}{\gamma_{\text{min}}}, \quad (8)$$

with  $\tilde{h}_{kk} = \mathbf{h}_k^H \mathbf{w}_k$ ,  $\tilde{h}_{ki} = \mathbf{h}_k^H \mathbf{w}_i$ , and  $\tilde{h}_{0k} = \mathbf{h}_0^H \mathbf{w}_k$ . We can now transform (7) into:

$$\rho_k \left( \sum_{\substack{i=1 \\ i \neq k}}^K |\tilde{h}_{ki} + \tilde{\mathbf{g}}_{ki}^H \boldsymbol{\phi}_r|^2 + \sigma_k^2 \right) - |\tilde{h}_{kk} + \tilde{\mathbf{g}}_{kk}^H \boldsymbol{\phi}_r|^2 \leq 0. \quad (9)$$

Thus, problem (6) can be reformulated as:

$$\max_{\boldsymbol{\rho}, \boldsymbol{\phi}_t, \boldsymbol{\phi}_r} r(\boldsymbol{\phi}_r) \quad (10a)$$

$$\text{subject to } |[\boldsymbol{\phi}_t]_n|^2 + |[\boldsymbol{\phi}_r]_n|^2 = 1 \quad \forall n \in \mathcal{N}, \quad (10b)$$

$$|[\boldsymbol{\phi}_t]_n|, |[\boldsymbol{\phi}_r]_n| \in [0, 1] \quad \forall n \in \mathcal{N}, \quad (10c)$$

$$(8), (9). \quad (10d)$$

To handle the non-convexity in (10b), we use the penalty method and problem (10) can be written as:

$$\max_{\boldsymbol{\rho}, \boldsymbol{\phi}_t, \boldsymbol{\phi}_r} r(\boldsymbol{\phi}_r) + C \sum_{n=1}^N (|[\boldsymbol{\phi}_t]_n|^2 + |[\boldsymbol{\phi}_r]_n|^2 - 1) \quad (11a)$$

$$\text{subject to } |[\boldsymbol{\phi}_t]_n|^2 + |[\boldsymbol{\phi}_r]_n|^2 \leq 1 \quad \forall n \in \mathcal{N}, \quad (11b)$$

$$|[\boldsymbol{\phi}_t]_n|, |[\boldsymbol{\phi}_r]_n| \in [0, 1] \quad \forall n \in \mathcal{N}, \quad (11c)$$

$$(8), (9). \quad (11d)$$

where  $C$  is a large positive constant that enforces  $|[\boldsymbol{\phi}_t]_n|^2 + |[\boldsymbol{\phi}_r]_n|^2 = 1$  for the optimal solution of (11). To handle the non-convex parts in (11a) and (9), we use the SCA method, and the objective in (11a) can be approximated as:

$$r(\boldsymbol{\phi}_r) + \underbrace{2C \sum_{n=1}^N \mathcal{R}([\boldsymbol{\phi}_t]_n^{(j-1)H} ([\boldsymbol{\phi}_t]_n - [\boldsymbol{\phi}_t]_n^{(j-1)})) + ([\boldsymbol{\phi}_r]_n^{(j-1)H} ([\boldsymbol{\phi}_r]_n - [\boldsymbol{\phi}_r]_n^{(j-1)}))}_{f(\boldsymbol{\phi}_t, \boldsymbol{\phi}_r)} \quad (12)$$

where  $f(\boldsymbol{\phi}_t, \boldsymbol{\phi}_r)$  is the first-order Taylor series of  $C \sum_{n=1}^N (|[\boldsymbol{\phi}_t]_n|^2 + |[\boldsymbol{\phi}_r]_n|^2 - 1)$  and the superscript  $(j-1)$  represents the value of the variables at iteration  $(j-1)$ . Likewise, using the SCA method, (9) can be expressed as:

$$\rho_k \left( \sum_{\substack{i=1 \\ i \neq k}}^K |\tilde{h}_{ki} + \tilde{\mathbf{g}}_{ki}^H \boldsymbol{\phi}_r|^2 + \sigma_k^2 \right) - |\tilde{h}_{kk} + \tilde{\mathbf{g}}_{kk}^H \boldsymbol{\phi}_r^{(j-1)}|^2 - 2\mathcal{R} \left( (\tilde{h}_{kk} + \tilde{\mathbf{g}}_{kk}^H \boldsymbol{\phi}_r^{(j-1)})^H \tilde{\mathbf{g}}_{kk}^H (\boldsymbol{\phi}_r - \boldsymbol{\phi}_r^{(j-1)}) \right) \leq 0, \quad (13)$$

where the later part of (13) is the first-order Taylor series evaluated at  $\boldsymbol{\phi}_r = \boldsymbol{\phi}_r^{(j-1)}$ . Eventually, the non-convex problem in (11) can be recast as follows:

$$\max_{\boldsymbol{\rho}, \boldsymbol{\phi}_t, \boldsymbol{\phi}_r} r(\boldsymbol{\phi}_r) + f(\boldsymbol{\phi}_t, \boldsymbol{\phi}_r) \quad (14a)$$

$$\text{subject to } (8), (11b), (11c), (13). \quad (14b)$$

Problem (11) can be solved using the SCA method, where the approximated convex problem in (14) is solved at each iteration.

### B. Beamforming Optimization at the BS

Given the transmission coefficients  $\boldsymbol{\phi}_t$  and reflection coefficients  $\boldsymbol{\phi}_r$ , the problem in (5) can be reformulated as:

$$\max_{\mathbf{W}, \boldsymbol{\eta}} \sum_{k=1}^K B \log_2(1 + \eta_k) \quad (15a)$$

$$\text{subject to } \eta_k \leq \frac{|\mathbf{z}_{rk} \mathbf{w}_k|^2}{\sum_{i=1, i \neq k}^K |\mathbf{z}_{rk} \mathbf{w}_i|^2 + \sigma_k^2} \quad (15b)$$

$$\sum_{k=1}^K |\mathbf{z}_{t0} \mathbf{w}_k|^2 + \sigma_0^2 \leq \frac{P_{\text{Rx}}}{\gamma_{\text{min}}}, \quad (15c)$$

$$\sum_{k=1}^K \|\mathbf{w}_k\|^2 \leq P_{\text{max}}, \quad (15d)$$

where  $\boldsymbol{\eta} = [\eta_1, \eta_2, \dots, \eta_K]$  is a slack vector which insures that constraint (15b) always holds with equality to the optimal solution,  $\mathbf{z}_{rk} = \mathbf{h}_k^H + \boldsymbol{\phi}_r^T \mathbf{G}_k$ , and  $\mathbf{z}_{t0} = \mathbf{h}_0^H + \boldsymbol{\phi}_t^T \mathbf{G}_0$ .

To handle the non-convexity in (15b), we introduce a new variable  $\zeta_k$  to decompose (15b) into

$$|\mathbf{z}_{rk} \mathbf{w}_k|^2 \geq \zeta_k \eta_k \quad (16)$$

and

$$\sum_{i=1, i \neq k}^K |\mathbf{z}_{rk} \mathbf{w}_i|^2 + \sigma_k^2 \leq \zeta_k \quad (17)$$

Noting that the term  $\mathbf{z}_{rk} \mathbf{w}_k$  in (16) can be seen as a real number with an arbitrary rotation of the beamforming vector  $\mathbf{w}_k$  [15], (16) will be equivalent to  $\mathcal{R}(\mathbf{z}_{rk} \mathbf{w}_k) \geq \sqrt{\zeta_k \eta_k}$ . By replacing the concave function  $\sqrt{\zeta_k \eta_k}$  with the first-order Taylor series, we can rewrite (16) as:

$$\mathcal{R}(\mathbf{z}_{rk} \mathbf{w}_k) \geq \sqrt{\zeta_k^{(j-1)} \eta_k^{(j-1)}} + \frac{1}{2} \sqrt{\frac{\zeta_k^{(j-1)}}{\eta_k^{(j-1)}}} (\eta_k - \eta_k^{(j-1)}) + \frac{1}{2} \sqrt{\frac{\eta_k^{(j-1)}}{\zeta_k^{(j-1)}}} (\zeta_k - \zeta_k^{(j-1)}). \quad (18)$$

Through these approximations, the non-convex problem in (15) can be approximated as the following convex problem:

$$\max_{\mathbf{W}, \boldsymbol{\eta}, \boldsymbol{\zeta}} \sum_{k=1}^K B \log_2(1 + \eta_k) \quad (19a)$$

$$\text{subject to } \zeta_k \geq 0 \quad \forall k \in \mathcal{K} \quad (19b)$$

$$(15c), (15d), (17), (18), \quad (19c)$$

---

**Algorithm 1:** Alternating Optimization using SCA
 

---

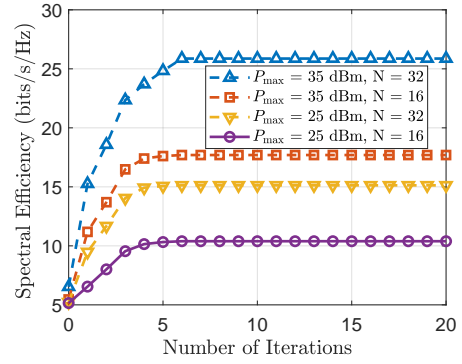
- Initialize:**  $\phi_t^{(0)}, \phi_r^{(0)}, \mathbf{W}^{(0)}$ . Set iterations to  $j = 1$ .
- 1 **repeat**
  - 2     Given  $\mathbf{W}^{(j-1)}$ , solve the transmission and reflection coefficients optimization problem in (6) using the SCA method to obtain  $\phi_t^{(j)}$  and  $\phi_r^{(j)}$ .
  - 3     Given  $\phi_t^{(j)}$  and  $\phi_r^{(j)}$ , solve the beamforming optimization problem in (15) using the SCA method to obtain  $\mathbf{W}^{(j)}$ .
  - 4     Set  $j = j + 1$ .
  - 5 **until** the objective (5a) converges;
- 

where  $\zeta = [\zeta_1, \zeta_2, \dots, \zeta_K]$ . Hence, the beamforming optimization problem in (15) can be solved using the SCA method, where the approximated convex problem in (19) is solved at each iteration. Hence, we obtain a convex optimization problem whose local optimum solutions can be reached through solving the preceding approximated problems iteratively. This problem can be efficiently solved using convex optimization solvers. The presented solution is detailed in Algorithm 1.

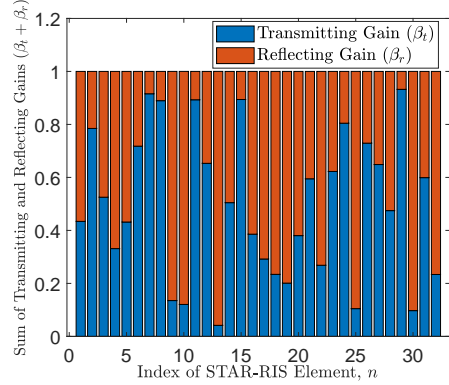
#### IV. SIMULATION RESULTS AND ANALYSIS

For our simulations, we consider a BS having  $M = 16$  directional antennas and  $K = 4$  secondary UEs. The location of the BS is fixed at (0,25,0), the location of the STAR-RIS is considered at (50,0,0), and the location of the primary Rx is considered at (60,5,0). We model the pathloss in dB as  $PL = 32.4 + 10c \log_{10}(d) + 20 \log_{10}(f)$  [16], where  $d$  is the distance between the transmitter and the receiver,  $f$  is the operating frequency, and  $c$  is the pathloss exponent set as  $c = 2$  for line-of-sight (LoS) and  $c = 5$  for non-line-of-sight paths [17]. Unless otherwise stated, we consider  $f = 28$  GHz,  $\gamma_{\min} = 20$  dB,  $B = 1$  MHz, and  $\sigma_k^2 = \sigma_0^2 = -174$  dBm/Hz [6]. Also, we assume that the channels are dominated by LoS paths.

We can express the channels between the BS and STAR-RIS as  $\mathbf{H} = \frac{\alpha}{\sqrt{PL}} \mathbf{a}_r(\theta^r, \psi^r) \mathbf{a}_t^H(\theta^t, \psi^t)$ , where  $PL$  is the pathloss between the BS and STAR-RIS,  $\alpha \in \mathbb{C}$  is the complex channel gain, and  $\mathbf{a}_r \in \mathbb{C}^{N \times 1}$  and  $\mathbf{a}_t \in \mathbb{C}^{M \times 1}$  are the normalized array response vectors at the STAR-RIS and BS, respectively [17]. Moreover,  $\theta^r, \psi^r$  and  $\theta^t, \psi^t$  are the azimuth/elevation angles of departure/arrival at the STAR-RIS and BS accordingly. In addition, we can express the channels from the BS to the UE as  $\mathbf{h}_k = \frac{\alpha_k}{\sqrt{PL_k}} \mathbf{a}_t(\theta_k^t, \psi_k^t)$ , where  $PL_k, \alpha_k, \theta_k^t,$  and  $\psi_k^t$  are defined similar to those of  $\mathbf{H}$ . The channel  $\mathbf{g}_k$  between the STAR-RIS and UE  $k$  is defined similar to  $\mathbf{h}_k$ . Then, we can define the cascaded channel  $\mathbf{G}_k = \frac{\alpha'_k}{\sqrt{PL'_k}} \text{diag}(\mathbf{g}_k^H) \mathbf{H}$ , where  $PL'_k$  and  $\alpha'_k$  are the pathloss and complex gain of the cascaded channel. Similar definitions hold for the primary network for  $\mathbf{h}_0, \mathbf{g}_0,$  and  $\mathbf{G}_0$ . We sample the UE positions within a circle of radius  $r = 5$  m from the STAR-RIS. All statistical results are averaged over a large number of independent runs. In our experiments, we compare



(a)



(b)

Fig. 2: a) Convergence behavior of the proposed algorithm, b) Sum of transmission and reflection coefficients for  $P_{\max} = 35$  dBm and  $N = 32$  elements.

the proposed STAR-RIS scheme with a conventional RIS that is modeled as a reflect-only RIS that is deployed adjacent to another transmit-only RIS [18]. To perform a fair comparison, each RIS is equipped with  $N/2$  elements.

Fig. 2a shows the convergence of the proposed STAR-RIS scheme for 4 combinations of simulation parameters over 20 iterations of the proposed solution. The simulation parameters herein are  $P_{\max} = 25$  and  $P_{\max} = 35$  dBm, and the number of STAR-RIS elements  $N = 16$  and  $N = 32$ . From Fig. 2a, we observe that the highest spectrum efficiency recorded was 25.87 bits/s/Hz that was achieved using  $P_{\max} = 35$  dBm and  $N = 32$  elements. In contrast, a minimal spectral efficiency of 10 bits/s/Hz is reached for  $P_{\max} = 25$  dBm and  $N = 16$  elements. Increasing  $P_{\max}$  and  $N$  for this minimal scenario by a factor 2, we can see that  $P_{\max}$  has a higher impact on the spectral efficiency that increases by around 70% recording 17 bits/s/Hz. In comparison, increasing  $N$  achieves around a 52% spectral efficiency increase that reaches 15.2 bits/s/Hz.

In Fig. 2b, we can see that the energy conservation is satisfied for all the indices of the STAR-RIS element. These values are reached after convergence of the proposed algorithm for  $P_{\max} = 35$  dBm and  $N = 32$  elements after 20 iterations. This result showcases how the uniquely dynamic transmission and reflection coefficient magnitudes assist in spectrum sharing, where both amplitudes and phases of the STAR-RIS coefficients can contribute to additional degrees of



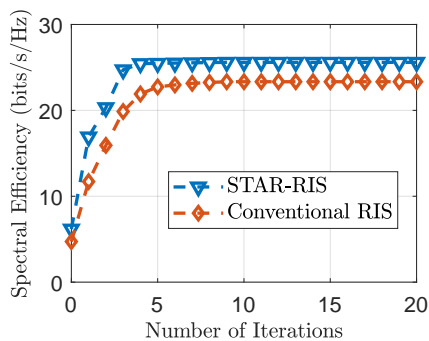


Fig. 3: Comparison of the achievable spectral efficiency between the STAR-RIS and the conventional RIS schemes having  $P_{\max} = 35$  dBm and  $N = 32$  elements.

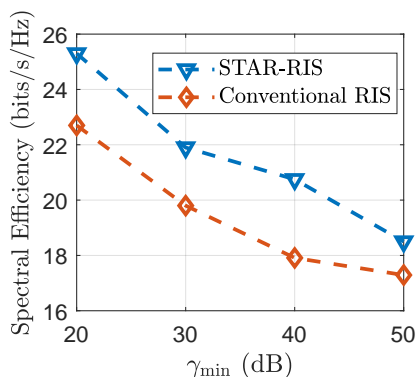


Fig. 4: Spectral efficiency achieved by the STAR-RIS and the conventional RIS schemes with  $P_{\max} = 35$  dBm and  $N = 32$  elements for different  $\gamma_{\min}$ .

freedom. This is in comparison to reflecting-only RISs which neglect the effect of the reflection coefficient magnitudes in spectrum sharing.

In Fig. 3, we can see that our proposed approach outperforms the conventional RIS scheme with  $P_{\max} = 35$  dBm and  $N = 32$  elements after convergence. In fact, the STAR-RIS dominates the conventional RIS performance for all iterations. Our proposed scheme achieves a spectral efficiency of 25.87 bits/s/Hz greater than that of the conventional RIS that reaches 22.58 bits/s/Hz after 20 iterations. Hence, the proposed scheme achieves a 14.57% spectral efficiency gain over the conventional RIS scheme.

In Fig. 4, we can see that our proposed STAR-RIS scheme achieves higher spectral efficiency in comparison to the conventional RIS scheme for different  $\gamma_{\min}$ . In particular, the STAR-RIS scheme records a maximum of 25.87 bits/s/Hz in comparison to 22.58 bits/s/Hz achieved by the conventional RIS at  $\gamma_{\min} = 20$  dB. Clearly, as  $\gamma_{\min}$  increases, the amplitude responses become more biased towards the primary network to guarantee the SINR requirement. Consequently, this directly impacts the QoS for the secondary UEs, where the spectral efficiency decreases noticeably. Although the spectral efficiency of both schemes drop with the increase of  $\gamma_{\min}$ , the proposed scheme was still able to achieve a better spectral efficiency of around 18.3 bits/s/Hz higher than that of the conventional RIS that reached 17.23 bits/s/Hz.

## V. CONCLUSION

In this paper, we have proposed a novel *STAR-RIS-aided mmWave spectrum sharing* solution to guarantee primary-secondary networks co-existence in B5G systems. In particular, a STAR-RIS topology is leveraged to transmit and reflect the incident signals simultaneously to manage interference and QoS demands separately. We have posed the STAR-RIS spectrum sharing problem as an optimization problem, where the STAR-RIS response coefficients and beamforming matrix at the BS are jointly optimized. Furthermore, the non-convex problem is solved using an alternating iterative algorithm. Numerical results show the superiority of the STAR-RIS-aided mmWave spectrum sharing scheme over a conventional RIS scheme in terms of spectral efficiency.

## REFERENCES

- [1] O. Semiari, W. Saad, M. Bennis, and M. Debbah, "Integrated millimeter wave and sub-6 GHz wireless networks: A roadmap for joint mobile broadband and ultra-reliable low-latency communications," *IEEE Wireless Communications*, vol. 26, no. 2, pp. 109–115, Apr. 2019.
- [2] M. Chen, U. Challita, W. Saad, C. Yin, and M. Debbah, "Artificial neural networks-based machine learning for wireless networks: A tutorial," *IEEE Communications Surveys & Tutorials*, vol. 21, no. 4, pp. 3039–3071, Oct.-Dec. 2019.
- [3] G. Hattab, E. Visotsky, M. Cudak, and A. Ghosh, "Toward the coexistence of 5G mmWave networks with incumbent systems beyond 70 GHz," *IEEE Wireless Communications*, vol. 25, no. 4, pp. 18–24, 2018.
- [4] S. Biswas, A. Bishnu, F. A. Khan, and T. Ratnarajah, "In-band full-duplex dynamic spectrum sharing in beyond 5G networks," *IEEE Communications Magazine*, vol. 59, no. 7, pp. 54–60, July 2021.
- [5] C. Casetti, "5G consolidates deployment by targeting new bands [mobile radio]," *IEEE Vehicular Technology Magazine*, vol. 16, no. 4, pp. 6–11, Dec. 2021.
- [6] Q. Zhang, W. Saad, and M. Bennis, "Millimeter wave communications with an intelligent reflector: Performance optimization and distributional reinforcement learning," *IEEE Transactions on Wireless Communications*, Mar. 2022.
- [7] M. Nemati, J. Park, and J. Choi, "RIS-assisted coverage enhancement in millimeter-wave cellular networks," *IEEE Access*, vol. 8, pp. 188 171–188 185, 2020.
- [8] J. He, K. Yu, Y. Zhou, and Y. Shi, "Reconfigurable intelligent surface enhanced cognitive radio networks," in *Proc. IEEE 92nd Vehicular Technology Conference (VTC2020-Fall)*, 2020, pp. 1–5.
- [9] J. Yuan, Y.-C. Liang, J. Joung, G. Feng, and E. G. Larsson, "Intelligent reflecting surface-assisted cognitive radio system," *IEEE Transactions on Communications*, vol. 69, no. 1, pp. 675–687, Jan. 2020.
- [10] P. Lai, H. Ding, L. Hu, F. Gong, and P. H. J. Nardelli, "Reconfigurable intelligent surface-enabled spectrum-sharing communications based on successive interference cancellation," *IEEE Wireless Communications Letters*, vol. 11, pp. 116–120, Jan. 2021.
- [11] X. Wang, Z. Fei, J. Guo, Z. Zheng, and B. Li, "RIS-assisted spectrum sharing between MIMO radar and MU-MISO communication systems," *IEEE Wireless Communications Letters*, vol. 10, no. 3, pp. 594–598, 2020.
- [12] M. Rihan and L. Huang, "Optimum co-design of spectrum sharing between MIMO radar and MIMO communication systems: An interference alignment approach," *IEEE Transactions on Vehicular Technology*, vol. 67, no. 12, pp. 11 667–11 680, 2018.
- [13] Y. Liu, X. Mu, J. Xu, R. Schober, Y. Hao, H. V. Poor, and L. Hanzo, "STAR: Simultaneous transmission and reflection for 360° coverage by intelligent surfaces," *arXiv preprint arXiv:2103.09104*, 2021.
- [14] X. Mu, Y. Liu, L. Guo, J. Lin, and R. Schober, "Simultaneously transmitting and reflecting (STAR) RIS aided wireless communications," *IEEE Transactions on Wireless Communications*, vol. 21, no. 5, pp. 3083–3098, 2021.
- [15] Z. Yang, M. Chen, W. Saad, W. Xu, M. Shikh-Bahaei, H. V. Poor, and S. Cui, "Energy-efficient wireless communications with distributed reconfigurable intelligent surfaces," *IEEE Transactions on Wireless Communications*, May 2021.
- [16] N. Docomo, "White paper on 5G channel model for bands up to 100 GHz," Tech. Rep., 2016. [Online]. Available: <http://www.5Gworkshops.com/SGCM.html>, Tech. Rep., 2016.
- [17] Y. Xiu, W. Sun, J. Wu, G. Gui, N. Wei, and Z. Zhang, "Sum-rate maximization in distributed intelligent reflecting surfaces-aided mmwave communications," in *Proc. IEEE Wireless Communications and Networking Conference (WCNC)*, May 2021, pp. 1–6.
- [18] C. Wu, X. Mu, Y. Liu, X. Gu, and X. Wang, "Resource allocation in STAR-RIS-aided networks: OMA and NOMA," *IEEE Transactions on Wireless Communications*, Mar. 2022.